

Initialization of NMR Quantum Registers using Long-Lived Singlet States

Soumya Singha Roy and T. S. Mahesh

*NMR Research Center,
Indian Institute of Science Education and Research (IISER),
Pune 411008, India*

(Dated: November 12, 2018)

An ensemble of nuclear spin-pairs under certain conditions is known to exhibit singlet state lifetimes much longer than other non-equilibrium states. This property of singlet state can be exploited in quantum information processing for efficient initialization of quantum registers. Here we describe a general method of initialization and experimentally demonstrate it with two-, three-, and four-qubit nuclear spin registers.

PACS numbers:

I. INTRODUCTION

It has been established theoretically that quantum systems are far more capable than their classical counterparts for certain computational tasks [1]. Although various types of quantum systems are being explored, the realization of a general purpose quantum processor remains a technological challenge [2]. Proof-of-principle type experimental demonstrations have been carried out for several problems including factorization, unsorted database search, and quantum simulations using Nuclear Magnetic Resonance (NMR) [3, 4]. Nuclear spins in an ensemble of molecules present a convenient architecture to simulate a quantum register. The practical demonstrations of Quantum Information Processing (QIP) using such registers are greatly benefited by the long coherence times of nuclear spins and the well developed control techniques of NMR [3, 4].

In order to carry out information processing, a quantum register must satisfy a set of criteria laid out by DiVincenzo [5]. An important criterion is the ability to precisely initialize the register to a desired ket of the computational basis. Nuclear spins in room temperature and at ordinary magnetic fields exist in a highly mixed state and therefore preparing a pure state is not straightforward [6–8]. The spin temperature can nevertheless be reduced by using parahydrogens [9] or by using Dynamic Nuclear Polarization [10]. In future, either or both of these techniques may be available for preparing NMR quantum registers into almost pure states [2]. The existing approach for initializing NMR registers is however based on specially prepared mixed states known as ‘pseudopure states’, which are isomorphic to pure states for several computational problems [11, 12].

Consider an ensemble of identical molecules each having n spin-1/2 nuclei in a magnetic field. The Zeeman Hamiltonian $\mathcal{H}_z = h \sum_j \nu_0^j I_z^j$, is characterized by the frequency ν_0^j of Larmor precession, and the z-component of the spin angular momentum operator I_z^j of spins $j = 1 \dots n$ [8]. In NMR-QIP, the eigenstates $|\pm 1/2\rangle$ of \mathcal{H}_z^j are labeled as $|0\rangle$ and $|1\rangle$ states of a qubit, and the multi-spin eigenbasis $\{|00 \dots 00\rangle, |00 \dots 01\rangle, \dots\}$ is treated as

the computational basis. In thermal equilibrium at ordinary room temperature T , the Boltzman factor kT is much larger than the Zeeman energy gaps, so that the density matrix can be expanded as

$$\rho_{\text{eq}} = 2^{-n} e^{-\mathcal{H}_z/kT} \approx 2^{-n} (\mathbb{1} + \rho_{\Delta}). \quad (1)$$

Here identity $\mathbb{1}$ corresponds to a background of uniformly populated levels and the trace-less part $\rho_{\Delta} = \sum_j \epsilon_j I_z^j$ is known as the deviation density matrix. The dimensionless numbers $\epsilon_j = -h\nu_0^j/kT$ have magnitudes $\sim 10^{-4}$ for protons in currently available magnetic fields at ordinary room temperatures. The deviation density matrix represents the unequal population distribution (over the uniform background) which lead to the observable magnetizations. Thus preparing a pure ground state i.e., $|000 \dots 0\rangle$ in an NMR quantum register is rather difficult. Nevertheless, Cory et al [11] and Chuang et al [12] have independently pointed out that often a pure state $|\psi\rangle\langle\psi|$ can be simulated by the pseudopure state

$$\rho_{\text{pps}} \approx 2^{-n} [(1 - \epsilon')\mathbb{1} + 2^n \epsilon' |\psi\rangle\langle\psi|]. \quad (2)$$

Here ϵ' is a measure of the magnetization retained in the pseudopure state and it usually gets halved with every additional qubit [13]. The unit background is invariant under the Hamiltonian evolution, does not lead to NMR signal and is ignored [11]. Thus the equilibrium density matrix of a single spin-1/2 nucleus is always in a pseudopure state. Initializing a multi-spin system into a pseudopure state however is essentially a non unitary process [4]. Several methods have earlier been proposed and they involved averaging of magnetization modes over the sample space (called ‘spatial averaging’ [14]) or over spin space (called ‘logical labeling’ [12, 15]) or over several transients (called ‘temporal averaging’ [16]). In some cases subsystem pseudopure states are easier to prepare either by transition selective pulses [17] or by coherence selection using pulsed field gradients [18], but these methods invariably result in loss of a qubit for further computation.

In the next section we propose a different approach that exploits long life-times of certain special states called ‘singlet states’. The following section details the exper-

imental demonstrations on model systems consisting of two, three and four-qubit NMR registers.

II. SINGLET STATES AND REGISTER INITIALIZATION

A. Singlet States

The Hamiltonian for an ensemble of spin-1/2 nuclear pairs of same isotope, in the RF interaction frame, can be expressed as

$$\mathcal{H}^{\text{eff}} = h \left[\frac{\Delta\nu}{2} I_z^1 - \frac{\Delta\nu}{2} I_z^2 + J I^1 \cdot I^2 + \nu_{12} I_x^{1,2} \right]. \quad (3)$$

Here the RF frequency is assumed to be at the mean of the two Larmor frequencies, and $\Delta\nu$, J and ν_{12} correspond respectively to the difference in Larmor frequencies (chemical shift difference), the scalar coupling constant and the RF amplitude (all in Hz). In the limiting case of $\Delta\nu \rightarrow 0$, the system is said to have magnetic equivalence, and the singlet state $|S_0\rangle = (|01\rangle - |10\rangle)/\sqrt{2}$, and the triplet states $|T_1\rangle = |00\rangle$, $|T_0\rangle = (|01\rangle + |10\rangle)/\sqrt{2}$, and $|T_{-1}\rangle = |11\rangle$ form an orthonormal eigenbasis of the internal Hamiltonian $\mathcal{H}_{\text{eq}}^{\text{eff}} = h J I^1 \cdot I^2$ [8].

The non-equilibrium nuclear spin states decay toward equilibrium state (1) with a time constant called ‘spin-lattice’ relaxation time constant T_1 [7]. Since most of the NMR experiments involve preparation and detection of non-equilibrium spin states, it was generally accepted that the duration of any NMR transient is limited by T_1 , although the theoretical limit of transverse relaxation is $2T_1$ [8]. Levitt and co-workers demonstrated that under the Hamiltonian $\mathcal{H}_{\text{eq}}^{\text{eff}}$ the decay constant of singlet state $|S_0\rangle$ is much larger than T_1 , and hence called it a long-lived state [19, 20]. The phenomenon is akin to the decoherence-free-subspace (DFS) which is well known in QIP [21]. Detailed theoretical analyses of singlet state decay have been provided by Levitt and co-workers [22, 23] and by Karthik and Bodenhausen [24]. The long life times of singlet states have been attributed to the fact that the singlet states are immune to the dominant intramolecular dipole-dipole relaxation mechanism, which is symmetric with respect to the exchange of spin states.

Experimentally, singlet decay constants upto $36T_1$ have been reported [25], and in another instance singlet lived till about half an hour [26]. Overcoming the T_1 limit has motivated a number of novel applications including studying slow molecular dynamics and transport processes [25, 27], precise measurements of NMR interactions [28], the transport and storage of hyper polarized nuclear spin order [29–34], homogeneous line narrowing in spectroscopy [35], and determining molecular torsion angles [36]. Recently we had reported that high-fidelity singlet states can be easily prepared and characterized in two-spin systems under various experimental conditions [37]. In the following we describe the preparation and

detection of singlet states and then elucidate the initialization of quantum registers.

B. Preparation and detection of singlet states

The state $|S_0\rangle\langle S_0| - |T_0\rangle\langle T_0|$ can be easily prepared from the equilibrium density matrix $I_z^1 + I_z^2$ by using the propagator

$$U_1^{1,2} = e^{-i\frac{\pi}{4}(I_z^1 - I_z^2)} e^{-i\frac{\pi}{2} I_y^{1,2}} e^{-i\frac{\pi}{2}(I_z^1 - I_z^2)} e^{-i\pi I_z^1 I_z^2} e^{-i\frac{\pi}{2} I_x^{1,2}}. \quad (4)$$

With certain approximations the above propagator can be constructed from the Hamiltonians similar to the one in (3) [38]. The equivalence Hamiltonian $\mathcal{H}_{\text{eq}}^{\text{eff}}$ may be realized by suppressing the chemical shift $\Delta\nu$ either by vanishing the Zeeman field [19], or by using a ‘spin-lock’ [20, 39]. In this work we employ the latter technique. The spin-lock may be achieved by applying a long low-power unmodulated RF [20], or by specially designed phase modulated sequence which were originally used for spin-decoupling [39].

The singlet states by themselves are inaccessible to macroscopic observables, but can be indirectly detected by removing the equivalence and transforming to observable single quantum coherence using the propagator [19, 20]

$$U_D^{1,2} = e^{-i\frac{\pi}{2} I_x^{1,2}} \cdot e^{-i\frac{\pi}{4}(I_z^1 - I_z^2)}. \quad (5)$$

Alternatively, a more detailed and quantitative analysis of singlet states may be carried out using density matrix tomography [37].

C. Initializing NMR Registers

The circuit for initializing a 2-qubit NMR register via singlet states is shown in Fig.1a. An initially imperfect singlet density matrix gets purified during the spin-lock period as a result of the long life time, while the artifact coherences are destroyed by relaxation process as well as the inhomogeneities in the spin-lock itself. There exist optimal spin-lock conditions at which one obtains singlet states with high fidelity [37]. Once the singlet state is prepared with high fidelity, the conversion $|S_0\rangle \rightarrow |01\rangle$ can be easily achieved by the propagator

$$U_2^{1,2} = e^{i\frac{\pi}{2} I_x^{1,2}} \cdot e^{-i\pi I_z^1 I_z^2} \cdot e^{-i\frac{\pi}{2} I_x^{1,2}}. \quad (6)$$

Finally a pulsed field gradient G_z can be used to destroy the residual single and multiple quantum coherences. If necessary, other pseudopure states can be obtained simply by applying NOT gates.

This procedure of initialization can be extended to multiqubit systems, since it is known that a spin-pair

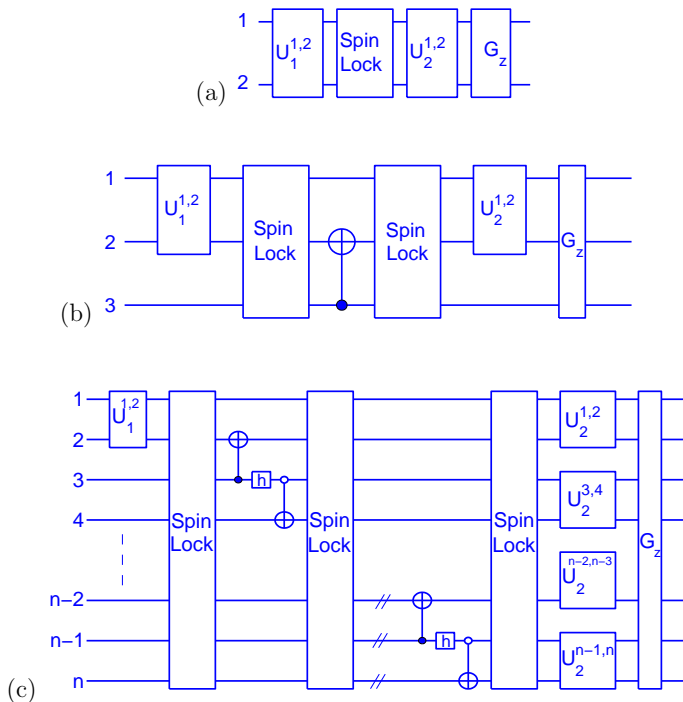


FIG. 1: The circuit diagrams for initializing (a) 2-qubit, (b) 3-qubit, and (c) n -qubit registers. In (c), the cNOT gates with open circles correspond to NOT operation if the control is 0 and identity if the control is 1. The h -gate corresponds to pseudo-Hadamard: $|0\rangle \xrightarrow{h} (|0\rangle - |1\rangle)/\sqrt{2}$ and $|1\rangle \xrightarrow{h} (|0\rangle + |1\rangle)/\sqrt{2}$.

may exhibit long-lived singlet state if it is situated sufficiently away from other spins [36]. The procedure of a 3-qubit initialization is shown in Fig.1b. We first prepare a two-qubit singlet and apply a cNOT gate on qubit-2 (controlled by qubit-3). Subsequent spin-lock and $U_2^{1,2}$ gate on qubits 1 and 2 initializes a three qubit system into $|010\rangle$ state. The circuit can be understood as follows. After preparing the singlet on qubits 1 and 2, the third qubit remains in a mixed state with a probability p_0 of being in state $|0\rangle$ and a probability p_1 of being in state $|1\rangle$. The cNOT gate transforms the mixed state according to:

$$|S_0\rangle\langle S_0| \otimes (p_0|0\rangle\langle 0| + p_1|1\rangle\langle 1|) \xrightarrow{\text{cNOT}} p_0|S_0\rangle\langle S_0| \otimes |0\rangle\langle 0| + p_1|\phi^-\rangle\langle \phi^-| \otimes |1\rangle\langle 1|. \quad (7)$$

First term in the output is singlet on qubits 1 and 2 and therefore survives during the second spin-lock where as the other term consisting of the Bell state $|\phi^-\rangle = (|00\rangle - |11\rangle)/\sqrt{2}$ decays fast. The singlet is ultimately transformed into $|01\rangle$ by $U_2^{1,2}$ and thus we obtain $|010\rangle$ pseudopure state with a good approximation.

A general scheme for the initialization of an n -qubit NMR quantum register is described in Fig.1c. The circuit can be analyzed in a similar way as in the 3-qubit case. The fact that only nearest-neighbor interactions are used is highly advantageous in practice. Experimentally, the

spin-lock of multiple singlet pairs can be achieved using sophisticated modulated RF sequences as described in the next section.

III. EXPERIMENTS

The following experiments are carried out in Bruker 500 MHz NMR spectrometer at an ambient temperature of 300 K. We used strongly modulated pulses for designing high fidelity local gates as well as cNOT gates [40, 41]. The spin-lock was achieved by WALTZ-16 - a phase modulated RF sequence, which is routinely used in broadband spin decoupling [37]. Spectra corresponding to pseudopure states are obtained by linear detection scheme using small flip angle RF pulses. Since the pseudopure states have one energy level more populated than the equal distribution in all others, the spectrum should consist ideally of only one transition per qubit in each case. Quantitative analyses of the pseudopure states are carried out using extended versions of density matrix tomography described in reference [37]. Finally, the success of the experimental state ρ in achieving a target pseudopure state ρ_{pps} is measured by calculating the correlation [40],

$$\langle \rho_{\text{pps}} \rangle = \frac{\text{trace}[\rho \cdot \rho_{\text{pps}}]}{\sqrt{\text{trace}[\rho^2] \cdot \text{trace}[\rho_{\text{pps}}^2]}}. \quad (8)$$

Often only the diagonal elements of the density matrices are relevant and in such cases, the ‘diagonal correlation’ can be expressed by replacing all the operators in the above expression by their diagonal parts. In the following we describe the individual cases of two-, three- and four-qubit registers.

A. 2-qubit register

The two-qubit system, Hamiltonian parameters, and the corresponding pseudopure and the reference spectra are shown in Fig.2(a-d). As shown in Fig.1a, the experiment involved preparing singlet using $U_1^{1,2}$, followed by RF spin-lock with amplitude 2 kHz and duration 12.4 s, which are optimized for high singlet content [37]. The decay constant for singlet state was 16.2 s approximately three times the T_1 values of the two spins. The singlet is then converted into $|01\rangle$ pseudopure state using $U_2^{1,2}$. A final gradient pulse served to destroy the artifact coherences. The bar plots showing the real and imaginary parts of the theoretical and experimental density matrix are shown in Fig.2(e-h). A very high correlation of 0.995 is obtained with $|01\rangle$ pseudopure state.

For some quantum algorithms a good starting point may be the singlet state itself, which can be extracted

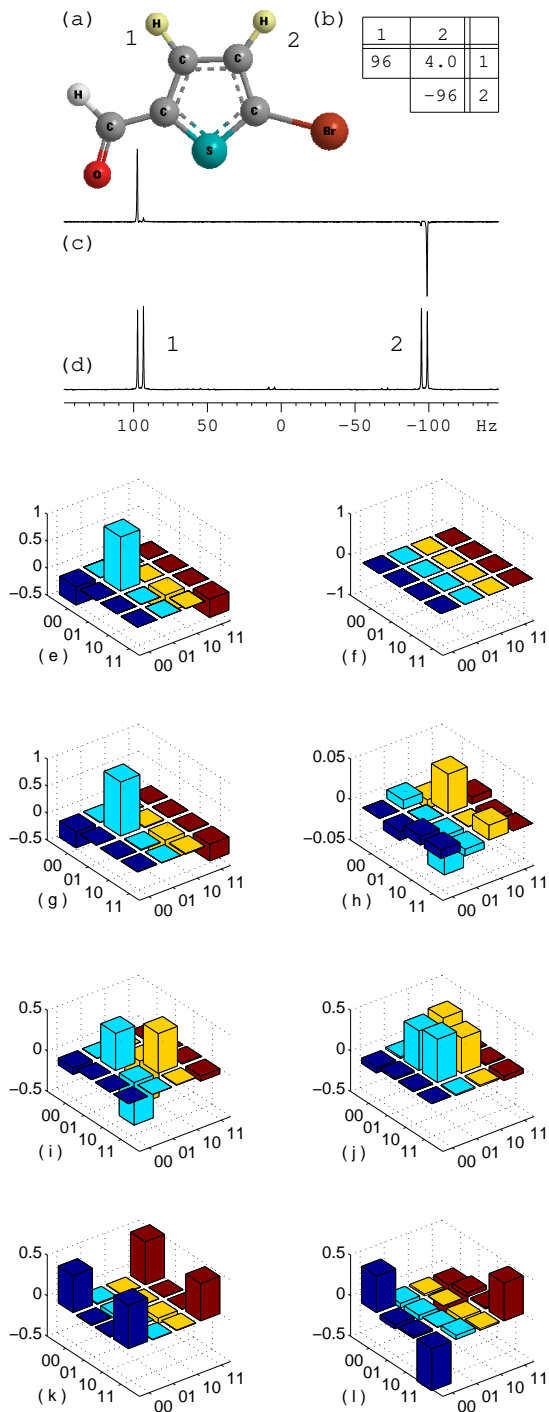


FIG. 2: The molecular structure (a) and Hamiltonian parameters (b) of 5-bromothiophene-2-carbaldehyde dissolved in CD_3OD , forming a homonuclear two-qubit register. In (b) diagonal and off-diagonal elements correspond to the chemical shifts and the scalar coupling constant respectively (in Hz). The ^1H spectra correspond to the pseudopure state (c) and the equilibrium mixed state (d). The barplots (e-h) correspond to the real (e,g) and imaginary (f,h) parts of theoretical (e,f) and experimental (g,h) pseudopure $|01\rangle$ state. The remaining barplots correspond to the experimental real parts of $|S_0\rangle$ (i), $|\psi^+\rangle$ (j), $|\phi^+\rangle$ (k), and $|\phi^-\rangle$ (l).

directly after the spin-lock shown in Fig.1a. The real part of the experimental singlet density matrix shown in Fig.2i has a correlation of 0.991. If necessary, initialization to other Bell states, starting from the singlet state, can be carried out easily:

$$\begin{aligned}
 |S_0\rangle &\xrightarrow{e^{i\pi I_z^1}} |\psi^+\rangle = (|01\rangle + |10\rangle)/\sqrt{2}, \\
 |S_0\rangle &\xrightarrow{e^{i\pi I_x^1} \cdot e^{i\pi I_z^1}} |\phi^+\rangle = (|00\rangle + |11\rangle)/\sqrt{2}, \\
 |S_0\rangle &\xrightarrow{e^{i\pi I_x^1}} |\phi^-\rangle = (|00\rangle - |11\rangle)/\sqrt{2}. \quad (9)
 \end{aligned}$$

The z-rotation in the above propagators can be implemented by simply chemical shift evolution for a period $1/(2\Delta\nu)$, and the qubit selective x-rotation can be implemented by using a strongly modulated pulse. The experimental density matrices corresponding to these Bell states have respective correlations 0.987 (Fig.2j), 0.982 (Fig.2k), and 0.968 (Fig.2l).

B. 3-qubit register

The three-qubit system, Hamiltonian parameters and the corresponding pseudopure and the reference spectra are shown in Fig.3(a-d). The decay constant for singlet state of spins 1 and 2 was about 18 s, approximately three times of their T_1 values. The pseudopure state was prepared using the circuit shown in Fig.1b. Each of the two spin-locks were achieved using 6.3 s of 500 Hz WALTZ-16 modulations. The cNOT gate was implemented using a 14 segment strongly modulated RF pulse of duration approximately 60 ms and of fidelity 0.96. The bar plots showing the real and imaginary parts of the theoretical and experimental density matrix are shown in Fig.3(e-h). The correlation of the experimental density matrix with the theoretical pseudopure state is $|010\rangle$ is 0.952. The correlation is smaller compared to the two-qubit case, mainly due to the errors in the cNOT gate. Nevertheless, the diagonal correlation is as high as 0.983.

C. 4-qubit register

The four-qubit system, Hamiltonian parameters and the corresponding pseudopure and the reference spectra are shown in Fig.4. The pseudopure state was prepared using the circuit shown in Fig.1c. The singlet decay constants were about 6 s, approximately twice the T_1 values of the individual spins. We were able to carry out simultaneous spin-lock of two singlet pairs and initialize a four-qubit register. The two spin-locks were achieved by 2 kHz WALTZ-16 modulations of durations 2 s and 4.5 s each. The two cNOT gates were made of 20 segments, approximately 61 ms duration and of fidelities about 0.94. The 10 segment h-gate was about 8.2 s long and of fidelity

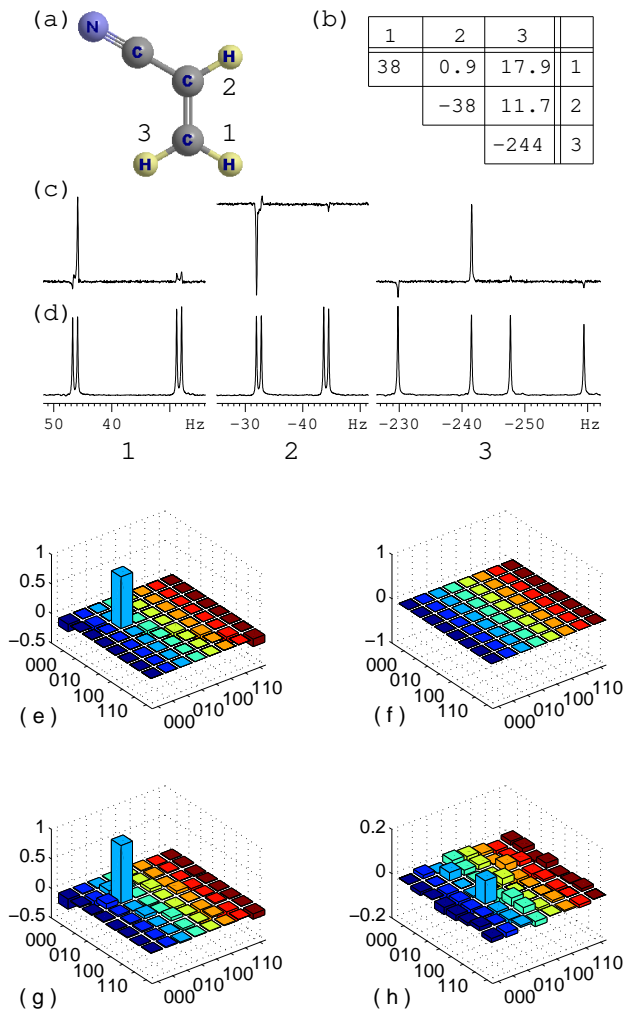


FIG. 3: The molecular structure (a) and Hamiltonian parameters (b) of acrylonitrile dissolved in CDCl_3 , forming a homonuclear 3-qubit register. In (b) diagonal elements are chemical shifts (in Hz) and the off-diagonal elements are the scalar coupling constants (in Hz). The ^1H spectra correspond to the pseudopure state (c) and the equilibrium mixed state (d). The bar plots are showing the real (e,g) and imaginary (f,h) parts of theoretical (e,f) and experimental (g,h) pseudopure $|010\rangle\langle 010|$ state.

0.98. Complete tomography of a 4-qubit density matrix is a laborious task. After the preparation of the pseudopure state, the non-zero quantum off-diagonal elements are efficiently destroyed by the final gradient pulse. Since only the diagonal elements are of main interest, we have carried out the four-qubit diagonal tomography [41]. The bar plot showing the diagonal part of the experimental density matrix is shown in Fig.4c. The diagonal correlation is estimated to be approximately 0.97 ± 0.01 with $|1001\rangle$ pseudopure state. The first pair has collapsed to $|10\rangle$ state instead of $|01\rangle$, due to an additional 180 degree pulse that was applied on qubits 1 and 2 for refocusing purposes during $U_2^{3,4}$.

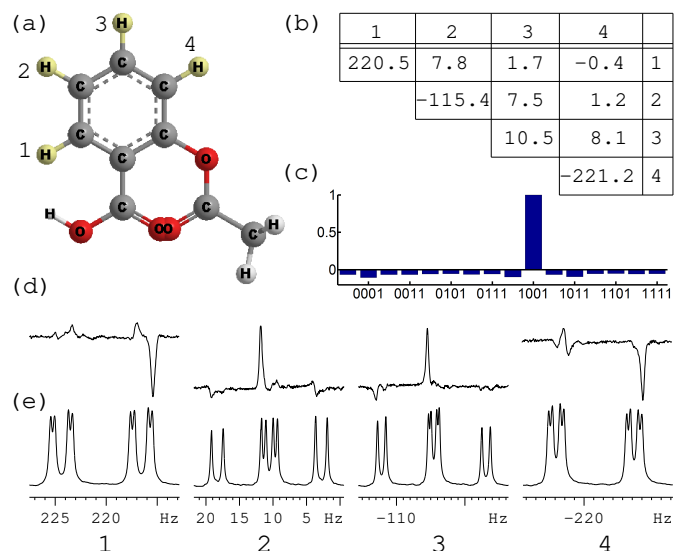


FIG. 4: The molecular structure (a) and Hamiltonian parameters (b) of aspirin dissolved in CD_3OD , forming a homonuclear 4-qubit register. In (b) diagonal elements are chemical shifts (in Hz) and the off-diagonal elements are the scalar coupling constants (in Hz). The barplot in (c) displays the diagonal elements of the density matrix obtained by tomography of the pseudopure $|1001\rangle$ state. The ^1H spectra correspond to the pseudopure state (d) and the equilibrium mixed state (e).

IV. CONCLUSIONS

We have demonstrated that robust initialization of NMR quantum registers are possible via long-lived singlet states. It is hard to initialize proton-based NMR registers using traditional methods. As a result many popular NMR registers were based on carbon spins or a combination of protons and carbons which permitted initialization by traditional methods. The proposed method of using long-lived singlet states enables us to initialize larger registers even though the long range interactions are weak. Molecules are of interest where in the inter pair dipolar couplings are sufficiently weak to keep the singlet states long-lived, while the covalent bond mediated scalar interactions among the nearest neighbor spins are sufficiently strong. Since para hydrogens naturally exist in singlet states, the method can be applied directly to the initialization of registers based on parahydrogens. While the register initialization is the first application of long-lived singlet states for QIP, more applications, like for example enhancing the memory of registers, may be realized in future. Similar techniques may be used for multi-qubit initialization in non-NMR systems exhibiting long-lived singlet states.

Acknowledgments

Authors gratefully acknowledge discussions with Prof. Anil Kumar and with Prof. G. S. Agarwal. The use of

500 MHz NMR spectrometer at NMR Research Center, IISER-Pune is also acknowledged.

-
- [1] M. A. Nielsen and I. L. Chuang, *Quantum Computation and Quantum Information*, Cambridge University Press (2002).
- [2] T. D. Ladd, F. Jelezko, R. Laflamme, Y. Nakamura, C. Monroe, and J. L. O'Brien, *Nature* **464**, 45 (2010).
- [3] C. Ramanathan, N. Boulant, Z. Chen and D. G. Cory, *Quant. Info. Proc.* **3**, 15-44 (2004).
- [4] D. Suter and T. S. Mahesh, *J. Chem. Phys.* **128**, 052206 (2008).
- [5] D. P. DiVincenzo, *Fortschr. Phys.* **48**, 771 (2000).
- [6] M. Goldman, *Spin Temperature and Nuclear Magnetic Resonance in Solids*, Oxford University Press (1970).
- [7] A. Abragam, *Principles of Nuclear Magnetism*, Oxford University Press (1961).
- [8] M. H. Levitt, *Spin Dynamics*, J. Wiley and Sons Ltd., Chichester (2002).
- [9] M. S. Anwar, J. A. Jones, D. Blazina, S. B. Duckett, H. A. Carteret, *Phys. Rev. A* **70**, 032324 (2004).
- [10] G. W. Morley, J. van Tol, A. Ardavan, K. Porfyrikis, J. Zhang, and G. A. D. Briggs *Phys. Rev. Lett.* **98**, 220501 (2007).
- [11] D. G. Cory, A. F. Fahmy, and T. F. Havel, *Proc. Natl. Acad. Sci. USA* **94**, 1634 (1997).
- [12] N. Gershenfeld and I. L. Chuang, *Science*, **275**, 350 (1997).
- [13] C. Negrevergne, T. S. Mahesh, C. A. Ryan, M. Ditty, F. Cyr-Racine, W. Power, N. Boulant, T. Havel, D. G. Cory, and R. Laflamme, *Phys. Rev. Lett.* **96**, 170501 (2006).
- [14] D. G. Cory, M. D. Price, and T. F. Havel, *Phys. D* **120**, 82 (1998).
- [15] K. Dorai, Arvind, and A. Kumar, *Phys. Rev. A* **61**, 042306 (2000).
- [16] E. Knill, I. L. Chuang, and R. Laflamme, *Phys. Rev. A* **57**, 3348 (1998).
- [17] T. S. Mahesh and A. Kumar, *Phys. Rev. A* **64**, 012307 (2001).
- [18] E. Knill, R. Laflamme, R. Martinez, and C. H. Tseng, *Nature* **404**, 368 (2000).
- [19] M. Carravetta, O. G. Johannessen, M. H. Levitt, *Phys. Rev. Lett.* **92**, 153003 (2004).
- [20] M. Carravetta and M. H. Levitt, *J. Am. Chem. Soc.* **126**, 6228 (2004).
- [21] D. A. Lidar and K. B. Whaley, *Irreversible Quantum Dynamics*, F. Benatti and R. Floreanini (Eds.), Springer Lecture Notes in Physics vol. 622, Berlin (2003); Also available at arXiv:quant-ph/0301032.
- [22] M. Carravetta and M. H. Levitt, *J. Chem. Phys.* **122**, 214505 (2005).
- [23] G. Pileio and M. H. Levitt, *J. Chem. Phys.* **130** (2009) 214501.
- [24] K. Gopalakrishnan and G. Bodenhausen, *J. Magn. Reson.* **182**, 254 (2006).
- [25] R. Sarkar, P. R. Vasos, and G. Bodenhausen, *J. Am. Chem. Soc.* **129**, 328 (2007).
- [26] G. Pileio, M. Carravetta, E. Hughes, and M. H. Levitt, *J. Am. Chem. Soc.* **130**, 12582 (2008).
- [27] S. Cavadini, J. Dittmer, S. Antonijevic and G. Bodenhausen, *J. Am. Chem. Soc.* **127**, 15744 (2005).
- [28] G. Pileio, M. Carravetta and M. H. Levitt, *Phys. Rev. Lett.* **103**, 083002 (2009).
- [29] A. K. Grant and E. Vinogradov, *J. Magn. Reson.* **193**, 177 (2008).
- [30] T. Jonischkeit, U. Bommerich, J. Stadler, K. Woelk, H. G. Niessen, and J. Bargon, *J. Chem. Phys.* **124**, 201109 (2006).
- [31] E. Y. Chekmenev, J. Hovener, V. A. Norton, K. Harris, L. S. Batchelder, P. Bhattacharya, B. D. Ross, and D. P. Weitekamp, *J. Am. Chem. Soc.* **130**, 4212 (2008).
- [32] P. R. Vasos, A. Comment, R. Sarkar, P. Ahuja, S. Jannin, J. P. Ansermet, J. A. Konter, P. Hautle, B. van den Brandt, and G. Bodenhausen, *Proc. Nat. Aca. Sci.* **106**, 18469 (2009).
- [33] R. W. Adams, J. A. Aguilar, K. D. Atkinson, M. J. Cowley, P. I. P. Elliott, S. B. Duckett, G. G. R. Green, I. G. Khazal, J. Lopez-Serrano, and D. C. Williamson, *Science* **323**, 1708 (2009).
- [34] W. S. Warren, E. Jenista, R. T. Branca, and X. Chen, *Science* **323**, 1711 (2009).
- [35] R. Sarkar, P. Ahuja, P. R. Vasos, and G. Bodenhausen, *Phys. Rev. Lett.* **104**, 053001 (2010).
- [36] M. C. D. Tayler, S. Marie, A. Ganesan and M. H. Levitt, *J. Am. Chem. Soc.* **132**, 8225 (2010).
- [37] S. S. Roy and T. S. Mahesh, *J. Magn. Reson.* (in press).
- [38] G. Pileio, M. Concistr, M. Carravetta, and M. H. Levitt, *J. Magn. Reson.* **182**, 353 (2006).
- [39] R. Sarkar, P. Ahuja, D. Moskau, P. R. Vasos, G. Bodenhausen, *ChemPhysChem* **8** 2652 (2007).
- [40] E. M. Fortunato, M. A. Pravia, N. Boulant, G. Teklemariam, T. F. Havel and D. G. Cory, *J. Chem. Phys.* **116**, 7599 (2002).
- [41] T. S. Mahesh and Dieter Suter, *Phys. Rev. A* **74**, 062312 (2006).